

On the energetics in the lower thermosphere

V P Bhatnagar^{§,*} & A Tan

Department of Physics, Alabama A & M University, Normal, AL 35762, U S A

[§]E-mail: vinbhatnagar@hotmail.com

Received 20 November 2009; revised 11 March 2010; re-revised 7 July 2010; accepted 13 July 2010

The resultant global mean heating rate due to solar EUV radiation in presence of the infrared cooling from the gases like carbon dioxide, nitric oxide and the atomic oxygen has been estimated in the altitude range 120 - 200 km for different solar activity and seasons at moderate latitudes utilizing MSIS-E models. The simplified energy equation leads to a peak height in the heating/cooling rates and a direct dependence of the exospheric temperature on these rates at the lower thermospheric boundary. The computations are performed mainly for quiet periods and steady state noon time maximum and nighttime minimum conditions, when the temperature variation with local time can be ignored. The increase in cooling rates in the lower thermospheric heights from increased densities tends to pull the exospheric temperature down and *vice versa*. However, during daytime the relative magnitudes of the heating and cooling rates determine the decrease in exospheric temperature. It is shown that ideally the heating/cooling rates above their peaks decrease with height exponentially [$\exp(-s(z - z_0))$], where, z , is the height; z_0 , the lower boundary; and s , a parameter dependent on the temperature profile and can be easily estimated from any model or observed temperatures. The case studies show that the resultant heating / cooling rates increase with increase in the solar activity / temperature irrespective of the season by a factor of about 2 from the minimum to maximum solar activity. The seasonally averaged heating rate values for daytime and nighttime at the peaks for moderate solar activity of about 0.7×10^{-7} and 0.9×10^{-7} (ergs $\text{cm}^{-3} \text{s}^{-1}$), respectively agree well with the existing theoretical and observed values. Above the peaks, the resultant average cooling rates during nighttime for quiet periods are larger by a factor of 2 to 8 depending on the solar activity from the observed ones just for nitric oxide by SABER instrument. This is probably due to the fact that SABER values include all local times, seasons, latitudes, longitudes and geophysical activities and does not include the main constituent, the atomic oxygen. The changes in the cooling rates from increased CO_2 and CH_4 could imply corresponding change in the atmospheric densities originating from related changes in the exospheric temperatures with resulting feedback to the cooling rates and subsequent density changes.

Keywords: Lower thermosphere, Exospheric temperature, Infrared cooling, Solar activity

PACS No: 92.60.hb

1 Introduction

The production of gases like carbon dioxide, methane and nitric oxide from natural gas, coal, oil and other human activities and increased human population, keeps increasing unabated since mid-fifties of the last century and poses a serious hazard for human, plant and animal population in the future to the world climate¹ with possible implications higher up in space. Just carbon dioxide has increased by about 30% since late 18th century and 20% since late fifties mainly due to increased population and anthropogenic emissions. The CO_2 (15 μm) cooling is dominant in the lowest thermosphere below ~130 km, while that from nitric oxide NO (5.3 μm) and atomic oxygen (O^3P , 62 μm) takes over above ~140 km. The implications of doubling and halving the concentration of greenhouse gases are well documented in the available literature for the troposphere² and in the stratosphere³.

The implications of the changes in the concentration of these gases for the thermosphere and the ionosphere have been summarized by Bougher *et al.*⁴ and Roble⁵. According to them, a doubling of the present day concentration of CO_2 and CH_4 mixing ratios at 120 km could cool the mesosphere and thermosphere by about 10 K and 50 K, respectively from present day conditions. As a result, thermospheric densities may decrease by 40 - 50 % of the present day values. The implications of these to the ionosphere have been discussed by Rishbeth & Roble⁶ using the National Center for Atmospheric Research (NCAR) thermosphere - ionosphere General Circulation Model (TIGCM). Such changes at higher altitudes also affect the satellite orbits and thus drag, and the numerous parameters deduced from satellite based instrumentations and other human activities in space.

Besides Mlynczak *et al.*^{7,8} studies on cooling for disturbed geophysical conditions only, there has not been much effort in estimating the variations in the resultant heating / cooling with respect to changes in the solar activity and the seasons in the thermosphere. Recently, a detailed study of radiative cooling by nitric oxide and carbon dioxide only for the declining phase of the solar cycle 23 from SABER instrument has been reported⁹, with which the results of the present study have been compared. Case studies have been presented to estimate such long term changes in the height variation of the resultant net heating rates during daytime and cooling rates during nighttime for these conditions from the simplified energy equation for noontime maximum and nighttime minimum conditions in temperature at thermospheric heights, when local time variation in the temperature can be ignored respectively. The method adopted in the present study yields analytical formulations to calculate the resultant mean rates from all the gases responsible like atomic oxygen, carbon dioxide and methane, and thus differentiates it from other works of Bougher & Roble¹⁰, and Mlynczak *et al.*⁸ which calculate for individual gases. In addition, the present study yields formulations in an analytic form the response of the exospheric temperature to such resultant heating/cooling rates in the lower thermosphere.

2 Theory

The global mean thermal balance equation in the vertical direction in the thermosphere is given as:

$$C\rho\left(\frac{\partial T}{\partial t} + v\frac{\partial T}{\partial z}\right) + p\frac{\partial v}{\partial z} = \frac{\partial}{\partial z}\left(AT^{0.69}\frac{\partial T}{\partial z}\right) + Q - L_e \quad \dots (1)$$

where, C , is the specific heat at the constant volume; T , the temperature; p , the pressure; ρ , the atmospheric density; and v , the mass averaged vertical transport velocity at height z . Here, $\frac{\partial T}{\partial t}$ is the horizontal local

time gradient and $\frac{\partial T}{\partial z}$ is the vertical gradient in the temperature at a certain height. $AT^{0.69}$ is the coefficient of molecular thermal conductivity¹¹; Q , the heating rate mainly by solar radiation, gravity waves and eddy thermal conductivity; and L_e , effective heat loss due to the infrared radiations from nitric oxide, carbon dioxide and atomic oxygen. The heating from thermal conduction becomes increasingly important above ~140 km. At mid latitudes and quiet geomagnetic

times considered here, the vertical velocity, v , is very small of the order of few ms^{-1} (ref. 12) with negligible height variation at moderate latitudes, hence, the product $p\frac{\partial v}{\partial z}$ can be easily neglected in comparison to the other terms. Following Vlasov¹³, $Q - L_e$ is replaced by jn , the net resultant heating where, j , is the average energy contribution per molecule in presence of solar EUV radiation and infrared radiations; and n , the number densities of the gases. Now Eq. (1) can be put as:

$$C\rho\left(\frac{\partial T}{\partial t} + v\frac{\partial T}{\partial z}\right) = A\frac{\partial}{\partial z}\left(T^{0.69}\frac{\partial T}{\partial z}\right) + jn \quad \dots (2)$$

where,

$$jn = Q - L_e \quad \text{(during daytime)} \quad \dots (2a)$$

$$jn = -L_e \quad \text{(during nighttime)} \quad \dots (3)$$

Therefore, jn is expected to be less during daytime than nighttime. In other words, Eqs (2a and 3) yields the average energy absorbed during daytime and essentially the heat loss by radiation during nighttime. The height profile of the temperature, T , in the thermosphere can be very well reproduced by an expression¹⁴:

$$T = T_\infty - (T_\infty - T_0)\exp[-s(z - z_0)] \quad \dots (4)$$

where, T_∞ , is the exospheric temperature; T_0 , temperature at z_0 the lower boundary; and s , parameter constant for a certain temperature profile. Also very small long term changes in temperature at 120 km are observed¹⁵, therefore, a lower boundary at 120 km is chosen. From Eq. (4):

$$\frac{\partial^2 T}{\partial z^2} = -s^2(T_\infty - T_0)\exp[-s(z - z_0)] \quad \dots (5)$$

Now substituting Eq. (5) in Eq. (2), one gets:

$$C\rho\left(\frac{\partial T}{\partial t} + v\frac{\partial T}{\partial z}\right) = -As^2T^{0.69}(T_\infty - T_0)\exp[-s(z - z_0)] + 0.69As^2T^{-0.31}(T_\infty - T_0)^2\exp[-2s(z - z_0)] + jn \quad \dots (6)$$

If one restrict oneself to maximum noontime (~1400 hrs LT) and minimum nighttime conditions (~0200 hrs LT) in temperatures at thermospheric heights, then the horizontal local time variation in temperature $\frac{\partial T}{\partial t}$ in Eq. (6) may be ignored, and is known as 'steady state equilibrium condition'. With the exception at very low heights where the term

$C_p v \frac{\partial T}{\partial z}$ can be of the order of other terms depending upon the magnitude of the velocity v , it becomes progressively negligible in comparison to the other terms at higher altitudes due to sharp decrease in the density and $\frac{\partial T}{\partial z}$. Therefore, in order to get a simplified analytical solution for j_n , if one neglects the LHS in Eq. (6), one gets:

$$j_n = A s^2 T^{0.69} (T_\infty - T_0) \exp[-s(z - z_0)] - 0.69 A s^2 T^{-0.31} (T_\infty - T_0)^2 \exp[-2s(z - z_0)] \dots (7)$$

Now Eq. (7) can easily be used to calculate the average resultant heating/cooling rates during daytime and nighttime, respectively for any temperature-height profile observed or from the models. The peak height z_m of j_n can be shown from Eq. (7) to be:

$$z_m = z_0 + 2.3 s^{-1} \log_{10} [1.4 (T_\infty - T_0) T^{-1}] \dots (8)$$

If one neglects temperature gradient in the upper thermosphere, then the second term on right side in Eq. (7) disappears and can be written at the lower boundary as:

$$T_\infty = T_0 + \frac{(Q - L_e)_0}{A s^2 T_a^{0.69}} \dots (9)$$

where, T_a is the average thermospheric temperature. The Eq. (9) gives the dependence of the exospheric temperature on $(j_n)_0$ at the lower boundary. It shows that an increase in cooling rates from increased CO₂ and CH₄ will tend to pull down T_∞ and *vice versa*, with other parameters held constant. However, the changes in T_∞ will depend on the relative magnitudes of Q and L_e .

3 Methodology

Computation of j_n from Eq. (7) requires knowledge of the parameter A , the thermal conductivity and s . The value of A was adopted at 56 for the predominant molecular oxygen and nitrogen at these heights¹¹. The temperature profiles in 120 - 200 km region for the present case studies were adopted from MSIS-E model¹⁶ for winter (15 January), summer (15 June) and equinox (15 March) of the year 2000 for moderate latitudes around (45°N, 45°E) for quiet periods. The parameter s was calculated from the best fit of Eq. (4) to the corresponding temperature profiles selected from the models. Thus, knowing T , s and T_∞ , the parameter j_n was calculated from Eq. (7) at

different heights for the solar minimum, moderate and maximum for noontime and nighttime conditions and seasons. The minimum, moderate and maximum solar activities are represented by 10.7 cm solar flux ($F_{10.7}$) of 70, 150 and 250×10^{-22} (Wm⁻² per Hz). Next, the dependence of the exospheric temperature / solar activity on the mean cooling rate in the height range 140 - 200 km, where NO and O are dominant, during nighttime is estimated.

4 Case studies

In Fig. 1, variation of the resultant $j_n (= Q - L_e)$ with height is shown for three solar activity conditions: the minimum, moderate and the maximum for the equinox (15 March) noontime around 1400 hrs LT for quiet geophysical conditions. The respective exospheric temperatures are 915, 1181 and 1268°K. In Fig. 2, similar calculations are shown for the noontime summer (15 June) with corresponding exospheric temperatures of 945, 1260 and 1400°K, respectively. Figure 3 shows the same for winter (15 January) noontime conditions with respective exospheric temperatures of 850, 1114 and 1210°K. Recent results show that the peaks in the heating and cooling rates occur around 130 - 140 km height respectively^{4,9,17} which agree with the present results. From these figures, it can be said that j_n decreases exponentially with height above the peaks as expected from Eq. (7). Irrespective of the seasons, the resultant net energy input rate increases by an average factor of up to 2.0 from solar minimum to maximum condition due to increase in solar activity or T_∞ . The daytime averaged heat input over all seasons at the peaks is about 0.7×10^{-7} ergs cm⁻³ s⁻¹ where the cooling from carbon dioxide predominates, during moderate solar

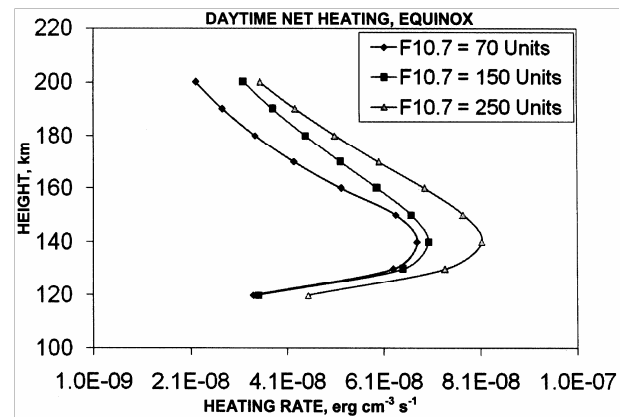


Fig. 1—Variation in mean daytime heating rates ($Q - L_e$) during equinox with height for solar minimum, moderate and maximum activities for quiet periods

activity, is close to the heating rate values of about 2.8×10^{-7} and 10^{-7} ergs $\text{cm}^{-3} \text{s}^{-1}$ of Gordiet's *et al.*¹⁷ at moderate solar activity and Roble & Emery's values¹⁸ at high solar activity, respectively.

The cooling rates ($j_n = L_e$) from infrared radiation have also been plotted with height for nighttime condition (~02 hrs LT) just for the equinox (Fig. 4). The increase is by a factor of up to 2 from solar minimum to maximum condition. During nighttime (Fig. 4), the average value of 0.9×10^{-7} ergs $\text{cm}^{-3} \text{s}^{-1}$ (present study) compares well with 0.6×10^{-7} reported at the peak height of 130 km as an average global cooling rate⁹ from SABER instrument. The increase in net heating/cooling during daytime and nighttime with solar activity is mainly due to increase in atmospheric densities with increase in solar activity.

Mlynczak *et al.*^{8,9} utilized the limb scanning radiometer SABER instrument on the NASA/TIMED

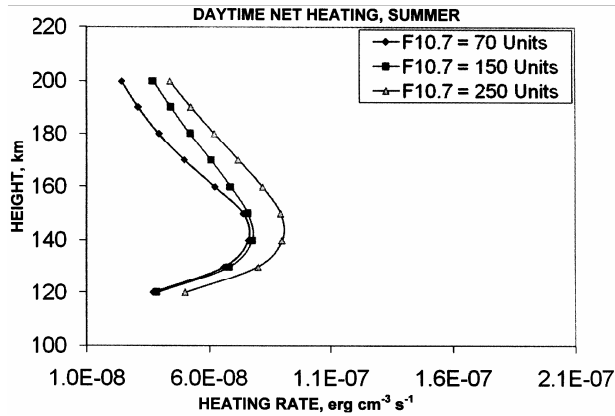


Fig. 2—Variation in mean daytime heating rates ($Q - L_e$) during summer with height for solar minimum, moderate and maximum activities for quiet periods

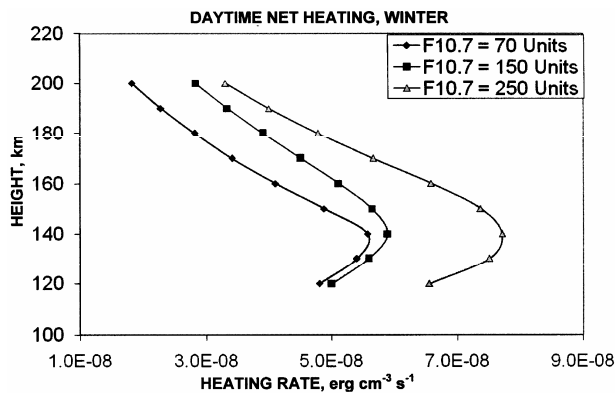


Fig. 3—Variation in mean daytime heating rates ($Q - L_e$) during winter with height for solar minimum, moderate and maximum activities for quiet periods.

satellite to study the height variation in the annual mean of the global infrared radiated power, cooling rates and fluxes during 2002 - 2008 by carbon dioxide and nitric oxide from the thermosphere. They found that these outputs decreased consistently with the declining phase of the solar cycle, in agreement with the present results. In Fig. 5, the variation of the mean infrared cooling rate j_n during nighttime for heights above 140 km, where the cooling from NO and O start to take over, is plotted against the solar flux as well as temperature. In the same figure, the average cooling rates from nitric oxide obtained from SABER are also plotted.

5 Results and discussion

In the present work, attempt has been made, under simplified assumptions, to present quantitatively the long term variations in the mean resultant

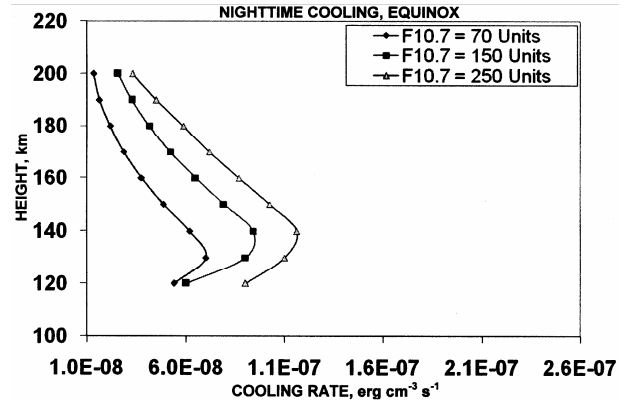


Fig. 4—Variation in mean nighttime infrared cooling rates (L_e) during equinox with height for solar minimum, moderate and maximum activities for quiet periods

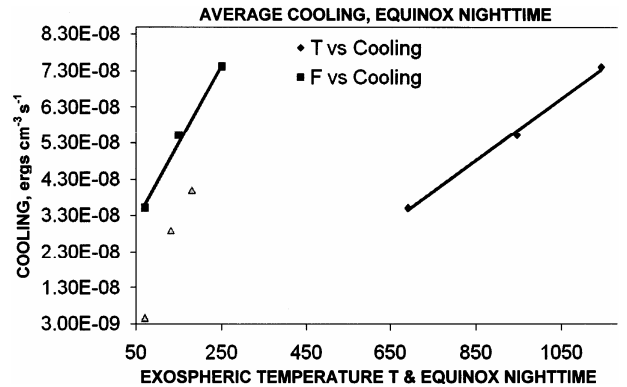


Fig. 5—Variation in the average nighttime cooling rates (L_e) above 140 km where nitric oxide and atomic oxygen predominate, during quiet periods with solar activity flux ($10^{-22} \text{ W m}^{-2} \text{ Hz}^{-1}$) and exospheric temperature (K). The SABER data (Δ) is average and includes all local times, latitudes, longitudes and all geophysical activities and no contribution from atomic oxygen

heating/cooling rates in presence of carbon dioxide, nitric oxide and atomic oxygen with solar activity and season for noontime and nighttime equilibrium conditions. Therefore, the treatment here is not suitable for short timescales of hours and during disturbed geophysical conditions. A linear dependence of the exospheric temperature/solar activity on these rates is also deduced. The limited analysis here for selected cases at moderate latitudes shows that during daytime the average net heating rates ($Q - L_e$) increase with increase in solar activity or exospheric temperature by a factor of up to 2.0 in 120 – 200 km range in the lower thermosphere. The calculated average daytime net heating rate over all seasons of about 0.7×10^{-7} ergs $\text{cm}^{-3} \text{s}^{-1}$ at the peaks for moderate solar activity compares well with the heating rates of 2.8×10^{-7} ergs $\text{cm}^{-3} \text{s}^{-1}$ and about 10^{-7} ergs $\text{cm}^{-3} \text{s}^{-1}$ obtained by Gordiet *et al.*¹⁷ and Roble & Emery¹⁸ for moderate and high solar activity, respectively. Also during nighttime (Fig. 4), a value of 0.9×10^{-7} ergs $\text{cm}^{-3} \text{s}^{-1}$ at the peak during equinox for moderate solar activity agrees with 0.6×10^{-7} reported as an average cooling rate at the peak height of 130 km (ref. 9) from SABER instrument.

Any increase in cooling rates (L_e) at the lower boundary with increase in CO_2 and CH_4 will tend to lower the exospheric temperatures associated with the solar activity and thus lower densities with feedback of decreased cooling and *vice versa*. This result agrees quantitatively with that obtained by Roble⁵ and Mlynczak *et al.*^{8,9}. However, during daytime any increase/decrease in exospheric temperature will depend on the relative magnitudes of the heating and cooling rates. At high latitudes and during active geomagnetic conditions, which are not dealt here, not only the Eq. (1), the whole situation becomes more complex as a result of enhanced nitric oxide for such conditions¹⁹⁻²¹. Such large changes in densities will drastically affect the exospheric temperature associated with a certain solar activity, which in turn will further perturb the densities with feedback to exospheric temperatures again.

Figure 5 shows the resultant average cooling rates in the 140 - 200 km region, where nitric oxide and atomic oxygen dominate for minimum, moderate and maximum solar activities and corresponding exospheric temperatures for quiet condition and equinox nighttime conditions. The present limited observed values during nighttime show almost a linear increase with solar activity and exospheric

temperature. This increase can be represented by the relation:

$$L_e \approx 0.02 F + 3.0 \quad \dots (10)$$

where, L_e , is in units of 10^{-8} ergs $\text{cm}^{-3} \text{s}^{-1}$ and F in units of 10^{-22} $\text{Wm}^{-2} \text{Hz}^{-1}$. The observed average values from nitric oxide in the 140 – 200 km range (triangles) from SABER/TIMED instrument⁹ have also been plotted for minimum (~ 70 units, year 2008), moderate (~ 130 units, year 2003) and maximum (~ 180 units, year 2002) solar activities. These values are lower by a factor in the range 2 - 8 depending on the solar activity. It may be due to the fact that the present values are only for mid latitudes, quiet periods and includes as well atomic oxygen. SABER values are averages including all local times, latitudes, longitudes and geomagnetic activities, and do not include atomic oxygen. Much more data analysis is needed now to quantify these differences and the detailed effects of the solar and geomagnetic activity and seasons on the cooling rates and the related changes in the densities of the contributing gases with resulting feedback to temperatures and densities.

6 Conclusions

On the basis of the simplified global mean thermal balance equation, the long term resultant heating/cooling rates from carbon dioxide, nitric oxide and atomic oxygen have been theoretically estimated in the 120–200 km region in the thermosphere at mid latitudes. The computations have been done for steady state daytime maximum (~ 1400 hrs LT) and nighttime minimum (~ 0200 hrs LT) conditions, when the horizontal local time variation in temperature can be ignored at thermospheric heights. The calculations have been performed for minimum, moderate and maximum solar activities, different seasons and quiet geomagnetic conditions. The significant results are summarized as:

- The exospheric temperature is theoretically tied to the heating/cooling rates at the lower boundary. An increase in cooling rates, say, by CO_2 and CH_4 tend to decrease the exospheric temperature and *vice versa*.
- The peak heights at around 130 to 140 km obtained agree well with the existing values.
- The heating/cooling rates above the peaks are shown theoretically to decrease exponentially with height in agreement with observations.

- (d) The heating/cooling rates at any height increase with increase in solar activity and hence, with exospheric temperature mainly due to increase in atmospheric densities. Irrespective of the seasons, the rates increase by a factor of up to 2.0 from solar minimum to maximum condition.
- (e) The seasonally averaged net heating rate at the peaks during daytime and nighttime are about 0.7×10^{-7} and 0.9×10^{-7} ergs $\text{cm}^{-3} \text{s}^{-1}$ during moderate solar activity and conform well with the existing values.
- (f) The average cooling rate above the peak shows a linear increase with increase in solar activity or exospheric temperature.
- (g) The present average cooling rates in 140–200 km range for quiet geomagnetic periods are larger by a factor of about 2 at moderate solar activity and about 8 at low solar activity than the SABER values for nitric oxide. It seems probably due to the fact that the SABER data includes all local times, latitudes, longitudes, geomagnetic activities, and does not include atomic oxygen and needs further investigation.
- (h) The known increase in nitric oxide drastically as compared to other constituents at high geomagnetic activities and at high latitudes (not dealt at present), and the uncertainties in carbon dioxide relaxation rates with temperature will further complicate the present scenario, besides making the energy equation more complex. Much more theoretical and data analysis is required to quantify this chain of events in the feedback loop.

Acknowledgements

The authors thank Drs M G Mlynczak and L A Hunt of NASA Langley Research Center, Hampton, VA, USA for supplying data from TIMED/SABER instrument. Preliminary results from this paper were presented at the AGU Spring in Fort Lauderdale, Florida, USA in 2008.

References

- Intergovernmental Panel for Climate Change (IPCC), *Fourth assessment report (AR4)*, Working Group 1 Report, 2007.
- Hansen J, Fung I, Lacis A, Rind D, Lebedeff S, Ruedy R, Russell G & Stone P, Global climate change as forecast by GISS three dimensional model, *J Geophys Res (USA)*, 93 (1988) 9341.
- Brasseur G, Hitchman M H, Simon P C & de Ruder A, Ozone reduction in the 1980's: A model simulation of anthropogenic and solar perturbations, *Geophys Res Lett (USA)*, 15 (1988) 1361.
- Bougher S W, Hunten D M & Roble R G, CO₂ cooling in the terrestrial planet thermospheres, *J Geophys Res (USA)*, 99 (1994), 14609.
- Roble R G, Major greenhouse cooling (yes, cooling): The upper atmosphere response to increased CO₂, US National Report 1991 – 1994, *Rev Geophys (USA)*, (1995) 539
- Rishbeth H & Roble R G, Cooling of the upper atmosphere by enhanced greenhouse gases: Modelling the thermosphere and ionospheric effects, *Planet Space Sci (UK)*, 40 (1992), 1011.
- Mlynczak M G, Martin-Torres F J, Crowley G, Kratz D P, Funke B, Lu G, Lopez-Puertas M, Russell III J M, Kozyra J, Mertens C, Sharma R, Gordley L, Picard R, Winick J & Paxton L, Energy transport in the thermosphere during the solar storms of April 2002, *J Geophys Res (USA)*, 110 (2005) A12S25.
- Mlynczak M G, Martin-Torres F J, Marshall B T, Earl Thompson R, Williams J, Turpin T, Kratz D P, Russell III J M, Woods T & Gordley L L, Evidence for a solar cycle influence on the infrared energy budget and radiative cooling of the thermosphere, *J Geophys Res (USA)*, 112 (2007) A12302.
- Mlynczak M G, Hunt L A, Marshall B T, Martin-Torres F J, Mertens C J, Russell III J M, Remsberg E E, Lopez-Puertas M, Picard R, Winick J, Wintersteiner P, Thompson R E & Gordley L L, Observations of infrared radiative cooling in the thermosphere on daily to multiyear timescales from the TIMED / SABER instrument, *J Geophys Res (USA)*, 115 (2010) A03309.
- Bougher S W & Roble R G, Comparative terrestrial planet thermosphere I: Solar cycle variation of global mean temperature, *J Geophys Res (USA)*, 96 (1991) 11045.
- Rees M H, *Physics and Chemistry of the Upper Atmosphere* (Cambridge University Press), 1989, Chap 6.
- Burns A G, Killeen T L & Roble R G, Processes responsible for the compositional structure of the thermosphere, *J Geophys Res (USA)*, 94 (1989) 3670.
- Vlasov M N, On the basic processes forming the long-term variations of the exospheric temperatures, *Geophys Res Lett (USA)*, 27 (2000) 489.
- COSPAR International Reference Atmosphere (CIRA), Committee on Space research, Working Group 4, Part 3 (Akademie Verlag, Berlin), 1972.
- Golitsyn G S, Semenov A L, Shefov N N, Fichkova L M, Lysenko E V & Perov S P, Long term temperature trends in the middle and upper atmosphere, *Geophys Res Lett (USA)*, 23 (1996) 1741.
- MSIS-E, COSPAR International Reference Atmosphere, Part 1: Thermosphere Model, D Rees, ed, *Adv Space Res (UK)*, 8 (5) (1988) 6.
- Gordiet B F, Kulikov Yu N, Markov M N & Marov M Ya, Numerical modeling of the thermospheric heat budget, *J Geophys Res (USA)*, 87 (1982) 4504.
- Roble R G & Emery B A, On the global mean temperature of the thermosphere, *Planet Space Sci (UK)*, 13 (1983) 597.
- Bhatnagar V P, Effects of the solar variability and geophysical events on the mesospheric nitric oxide,

- Environment Canada Report# APRB-2-D1*, (Toronto, Canada), 1975.
- 20 Barth C A, Mankoff K D, Bailey S M & Solomon S C, Global observations of nitric oxide in the thermosphere *J Geophys Res (USA)*, 108 (2003) 1027.
- 21 Saetre C, Stadsnes J, Nesse H, Aksnes A, Petrinec S M, Barth C A, Baker N, Vondrak R R & Ostgaard N, Energetic electron precipitation and the nitric oxide abundance in the upper atmosphere: A direct comparison during geomagnetic storm, *J Geophys Res (USA)*, 109 (2004) A09302.